Journal of Electromyography and Kinesiology 72 (2023) 102810

Contents lists available at ScienceDirect

Journal of Electromyography and Kinesiology

journal homepage: www.elsevier.com/locate/jelekin

Surface electromyographic frequency characteristics of the quadriceps differ between continuous high- and low-torque isometric knee extension to momentary failure

Jonathan Murphy [a], Emma Hodson-Tole [b], Andrew D. Vigotsky [c], Jim R. Potvin [d], James P. Fisher [a], James Steele [a,*]

[a] Solent University, Department of Sport and Health, Southampton, UK
[b] Manchester Metropolitan University, Musculoskeletal Sciences and Sports Medicine Research Centre, Manchester Institute of Sport, Manchester, UK
[c] Northwestern University, Evanston, IL, USA
[d] McMaster University, Hamilton, ON, Canada

ARTICLE INFO

Keywords:
sEMG
Wavelets
Resistance training
Motor unit

ABSTRACT

Surface EMG (sEMG) has been used to compare loading conditions during exercise. Studies often explore mean/median frequencies. This potentially misses more nuanced electrophysiological differences between exercise tasks. Therefore, wavelet-based analysis was used to evaluate electrophysiological characteristics in the sEMG signal of the quadriceps under both higher- and lower-torque (70 % and 30 % of MVC, respectively) isometric knee extension performed to momentary failure. Ten recreationally active adult males with previous resistance training experience were recruited. Using a within-session, repeated-measures, randomised crossover design, participants performed isometric knee extension whilst sEMG was collected from the vastus medialis (VM), rectus femoris (RF) and vastus lateralis (VL). Mean signal frequency showed similar characteristics in each condition at momentary failure. However, individual wavelets revealed different frequency component changes between the conditions. All frequency components increased during the low-torque condition. But low-frequency components increased, and high-frequency components decreased, in intensity throughout the high-torque condition. This resulted in convergence of the low-torque and high-torque trial wavelet characteristics towards the end of the low-torque trial. Our results demonstrate a convergence of myoelectric signal properties between low- and high-torque efforts with fatigue via divergent signal adaptations. Further work should disentangle factors influencing frequency characteristics during exercise tasks.

1. Introduction

The electrophysiological characteristics of human motor units (MUs) during exercise tasks have historically been examined using electromyography (EMG) (Hodson-Tole and Wakeling, 2009; Duchateau and Enoka, 2011). A particular area of interest has been the role of external resistance magnitude (i.e., heavier or lighter loads) and thus force requirements in determining the characteristics of the EMG signal. Several recent studies have used surface EMG (sEMG) to compare the myoelectric activity between light and heavy resistance exercise tasks (Schoenfeld et al., 2014; Jenkins et al., 2015; Looney et al., 2016; Schoenfeld et al., 2016; Gonzalez et al., 2017; Chapman et al., 2019). In general, these studies observed that both mean and peak sEMG amplitudes are higher when resistance exercise is performed using higher loads (Schoenfeld et al., 2014b; Jenkins et al., 2015; Looney et al., 2016; Schoenfeld et al., 2016; Gonzalez et al., 2017). Although, in some instances, peak amplitudes—particularly at the point of momentary failure—appear similar (Schoenfeld et al., 2016; Gonzalez et al., 2017; Chapman et al., 2019). However, amplitude-based analyses alone only reveal one aspect of the EMG signal and, along with the nonstationarity

Abbreviations: CI, Compatibility interval; EMG, Electromyography; MVC, Maximal voluntary contraction; MU, Motor units; RF, Rectus femoris; SD, Standard deviation; sEMG, Surface Electromyography; VL, Vastus lateralis; VM, Vastus medialis.

* Corresponding author at: Faculty of Sport, Health, and Social Sciences, Southampton Solent University, East Park Terrace, Southampton, Hampshire SO14 0YN, UK.

E-mail address: james.steele@solent.ac.uk (J. Steele).

https://doi.org/10.1016/j.jelekin.2023.102810
Received 23 August 2022; Received in revised form 21 July 2023; Accepted 2 August 2023
Available online 2 August 2023

(i.e., ergodicity) of processes producing the EMG signal, renders the understanding of MU behaviours during exercise a challenge.

The EMG signal contains multiple frequencies, yet traditional analysis of sEMG frequency components in exercise typically considers mean or median frequency values, where all frequency components are banded together (e.g., Jenkins et al., 2015); however, this limits understanding of the aetiology of these mean/median frequency shifts (e.g., a reduction in mean frequency could reflect an increase in lower frequency components or a decrease in higher frequency components). One approach that overcomes some of the limitations of traditional sEMG frequency analysis is a wavelet-based analysis of frequency components. This technique was proposed by von Tscharner (2000) and has been successfully used in a range of applications (von Tscharner, 2002; von Tscharner & Goepfert, 2006; Wakeling & Rozitis, 2004; Hodson-Tole & Wakeling, 2007; Lee et al., 2011; Wakeling et al., 2001; Wakeling, 2009a; Wakeling, 2009b). Whilst there is debate about the physiological inferences that can be drawn from wavelet characteristics (e.g., motor unit recruitment and fibre types; von Tscharner and Nigg, 2008; Farina, 2008), wavelets may offer additional insight regarding the complexity of the sEMG signal. Whilst multiple factors may drive changes in frequency characteristics, differences under different task conditions (e.g., force requirements) may indicate at least some physiological differences. As such, explorative research aimed at describing the range of frequencies in the sEMG signal using wavelet analysis may identify differences, or indeed similarities, that prompt further research aimed at identifying physiological explanations.

Wavelet analysis quantifies signal power within defined frequency bandwidths, enabling a finer-grained assessment of the interplay between low- and high-frequency components and how they change over time (Hodson-Tole and Wakeling, 2009; Lee et al., 2011). This approach has been applied to endurance-type modes of exercise tasks to examine differences in intensities of effort (Graham et al., 2015), yet not to the commonly employed resistance exercise model. As prior research has explored the impact of force requirements in resistance exercise using only amplitude or mean/median frequency analyses of the sEMG signal, the current study aimed to explore and describe the multiple frequency components of the sEMG signal of the quadriceps using a wavelet-based analysis, recorded under both higher- and lower-torque (70 % and 30 % of maximal voluntary contraction [MVC], respectively) isometric knee extension, performed to momentary failure.

2. Methods

2.1. Experimental design

A within-session, repeated-measures, randomised crossover design was adopted to examine and compare frequency characteristics of the sEMG signal during isometric knee extensions with both high- and low-torque performed to momentary failure. The study was approved by the Centre of Health, Exercise and Sport Science Research Ethics Committee (ID No. 582) meeting the ethical standards of the Helsinki declaration and was conducted within the Sport Science Laboratories at Solent University.

2.2. Participants

A convenience sample of 10 recreationally active adult males (height: 179.6 ± 6.0 cm; mass: 76.8 ± 7.3 kg; age: 26 ± 7 years) with previous resistance training experience (6 ± 3 years) were recruited. Sample size was resource constrained by time[a] and availability of participants during the time under which the study was conducted. Exclusion criteria were based upon illness or any contraindications to physical activity identified using a physical activity readiness questionnaire, though no one was excluded. All participants read a participant information sheet, were afforded the opportunity to ask any questions, and then completed informed consent forms before any testing commenced.

2.3. Equipment

Stature was measured using a wall-mounted stadiometer (Harpenden stadiometer, Holtain Ltd, UK) and body mass was measured using balance scales (Seca 710 flat scales, UK). Trials were performed on an isokinetic dynamometer (Humac Norm, CSMi, USA). Surface electromyography was measured using a Trigno Digital Wireless sEMG System (Delsys, USA) and sensors with a 10 mm inter-electrode spacing. Torque and sEMG signals were collected using the isokinetic dynamometer and sEMG systems, respectively, which were synced using a Trigno Analogue Adaptor (Delsys, USA); both torque and sEMG signals were recorded using the EMGworks Acquisition software (Delsys, USA).

2.4. Testing

Two different conditions were examined: single continuous isometric efforts to momentary failure at 30 % MVC and at 70 % MVC using the right limb. Both conditions were counterbalanced between participants as to whether they would perform either the 30 % or 70 % condition first, separated by a 20-minute rest. Prior to each condition, MVCs were performed and participants were instructed to apply maximal isometric effort against a fixed resistance at 45° of knee flexion. This procedure was completed before each condition to determine the respective absolute torque demands for each participant that equated to 30 % and 70 % of MVC; that is to say, each trial was normalised to the preceding MVC. Participants were instructed to gradually build up to a maximal effort over 3 s and were instructed to gradually reduce their effort once it was clear that a maximal torque had been achieved (i.e. when the torque reading was no longer increasing). In all conditions, knee angle was set at 45° flexion (0° = full extension) to standardise the exercise between participants. Before testing started, participants completed a standardised warm up of 20 body weight squats.

Each participant was instructed to perform an isometric effort with enough torque to reach their respective target torque for each condition. Participants were provided with a visual aid in the form of a horizontal on-screen torque bar with limits set at 70 ± 5 % and 30 ± 5 % of MVC for the high- and low-torque conditions, respectively. Participants were instructed to generate enough torque to ensure a vertical on-screen torque bar was between the lower- and upper-limits until momentary failure. Participants were verbally encouraged throughout; if they fell below the lower torque limit, they were encouraged to attempt to regain their set torque output. Momentary failure was defined as when participants could no longer generate enough torque to keep within the torque limits set, despite exerting maximal effort (Steele et al., 2017), for > 5 s or more.

2.5. Surface Electromyography

sEMG was recorded (2000 Hz) during each condition from the vastus medialis (VM), rectus femoris (RF) and vastus lateralis (VL). Electrode placement was made according to recommendations from the Surface Electromyography for the Non-invasive Assessment of Muscles (SENIAM) project (http://www.seniam.org/). The electrode for the VM was placed at 50 % of the line from the anterior spina iliaca superior to the superior part of the patella and in the direction of this line. The electrode placement for the RF was perpendicular and at 80 % of the line between the anterior spina iliaca superior and the joint space in front of the anterior order of the medial ligament. The electrode for the VL was placed at 2/3 of the line from the anterior spina iliaca superior to the lateral side of the patella and in the direction of the muscle fibres. Participants' skin was shaved and cleaned using an alcohol-free cleansing wipe at the site used for electrode placement. Each electrode

[a] As this study was conducted as part of a student dissertation.

was secured using double sided sticky tape.

2.6. Wavelet based analysis

Myoelectric signals were decomposed into intensities as a function of time and frequency using an EMG-specific wavelet transformation (von Tscharner, 2000). A filter bank of 11 non-linearly scaled wavelets ($k \in \{0, 1, \cdots, 10\}$), with central frequencies (f_c) spanning 6.90–395.46 Hz, was used[b]. To quantify features of signal amplitude, the total intensity at each time point (I_t) was calculated by summing the intensities over wavelets $1 \leq k \leq 10$. Exclusion of the first wavelet ($k = 0$) ensures low-frequency content, associated with factors such as movement artefact, were not included in the analysis. The total intensity calculated is equal to twice the square of the root mean square value and further, the intensity spectra across the wavelets is equivalent to the power spectra of the sEMG signal calculated by Fourier transform (Wakeling et al., 2001).

To quantify changes in signal content within each frequency domain, changes in the intensity within each domain were calculated. Within each wavelet domain, an intensity ($I_{j,k}$) was calculated for each sample point (j). During the trials, the intensity changed as a function of trial duration. The rate of change was calculated as the slope of the linear least squares fit of log I_k plotted as a function of trial duration (0 to 1, representing the beginning and end of the trial, respectively). This describes the exponential change, expressed as the percentage change of I_k per trial.

In addition, the mean signal frequency ($\bar{f}$) of each trial was calculated to facilitate a more direct comparison with previous literature, wherein mean or median frequency analyses are reported. This also enabled us to contrast the mean frequency results with those from our wavelet-based analyses. Here, mean frequency was calculated from wavelet transformed data ($k = 1 - 10$) using the weighted mean,

$$\bar{f} = \frac{\Sigma_k f_c(k) I_k}{\Sigma_k I_k}$$

for both the start and end of the trials. The start and end of the trial was defined by torque thresholds of 25 % (start) and 75 % (end) of the mean torque throughout the trial to remove the effects of the ramping up/down of torque at the start/end of the trials i.e., the start of the trial for the purpose of analysis was defined as when participant had exceeded 25 % of the target torque, and the end when they had dropped below 75 %. The changes in signal intensity within each frequency domain was calculated between these two points. All analysis of EMG data was performed in Mathematica (version 11.1, Wolfram).

2.7. Statistical analysis

All code and data used for this study are available on the Open Science Framework (https://osf.io/g2z4w/). To assess the effects of torque on the myoelectric signal, we performed statistical analysis in R (version 4.0.2; R Core Team, 2020). Before performing inferential analyses to answer our research question, we first visually inspected and quantified the effects of set order and condition on MVC and time to momentary failure. These were considered descriptive analyses and are presented using individual data points and mean ± SD or geometric mean ⋇ geometric SD. Descriptions of trial durations and their differences were performed on the geometric (log) scale, and as such, are presented multiplicatively.

Our first analysis compared the mean frequency at momentary failure between the two torques (30 vs. 70 % MVC), after adjusting for initial mean frequency. We created a linear mixed-effects model that was parameterized as follows:

$$\bar{f}_{ij}^{End} = (\beta_{00} + u_{0j}) + \beta_{20} Condition_{ij} + e_{ij}$$

for row i in participant j, and where u_{0j} is a random effect for participant j, $\bar{f}$ is mean frequency, and *Condition* is dummy-coded 0 for 30 % and 1 for 70 % MVC. Each muscle was fit in a separate model due to convergence issues when attempting to fit them together. Since the residuals were not normally distributed, compatibility intervals (CI) for the effect of condition (β_{20}) were generated using the basic (reverse percentile) bootstrap with 500 replicates.

Second, we investigated the effects of torque on relative changes in wavelet intensities. We created a linear mixed-effects model in which we parameterized a mean-centred log(f) to linearize the relative change-frequency relationship. The resulting mixed-effects model, in Pinheiro-Bates-modified Wilkinson-Rogers notation (Wilkinson and Rogers, 1973; Pinheiro and Bates, 2000) for brevity's sake, was.

I ~ Muscle * Freq * Condition + (Freq + Condition + Muscle | Participant),

where Condition was dummy-coded 0 for 30 % and 1 for 70 % MVC. The mean-centring of the log(f) decreased collinearity between random effects, allowed for our intercepts to be interpretable, and enabled the model to converge on a solution with normally distributed and homoscedastic residuals. Thus, we parametrically calculated the CIs using estimated marginal means on the fixed effects (as a function of frequency, conditional on muscle and torque condition) and their contrasts with Satterthwaite degrees-of-freedom approximation (Lüdecke, 2018; Lenth, 2020).

Finally, we quantified the degree of wavelet similarity over time. Each high- and low-torque trial was respectively summarized by a 10 (wavelets) × 1000 (time points) matrix, with which we generated a 1000 × 1000 concordance cross-correlation matrix for each muscle for each participant (Vigotsky, 2020). For example, a participant's VM wavelet intensities from the 30 % and 70 % trials were used to generate a 1000 × 1000 matrix, with each element corresponding to the absolute agreement in wavelet intensities between time i in the 30 % trial and time j in the 70 % trial, and where agreement was quantified using Lin's concordance correlation coefficients. We used linear mixed-effects models to summarize these concordance correlation matrices. Three models—one for each muscle—quantified the effect of trial duration on wavelet intensity agreement, wherein the percentages of trial duration of the 30 % and 70 % conditions were used as regressors and the concordance correlation coefficient (ρ^c) at that time point was the response variable,

$$\rho_{ij}^c = (\beta_{00} + u_{0j}) + (\beta_{10} + u_{1j}) t_{ij}^{30\%} + (\beta_{20} + u_{2j}) t_{ij}^{70\%} + e_{ij}$$

We allowed slopes and intercepts to vary and we report parameter estimates (fixed-effects) along with participant-level variances (random-effects).

In addressing our research questions, we took an estimation approach rather than hypothesis-testing approach since we were neither interested in dichotomizing our findings nor comparing them to a null model (Gardner and Altman, 1986; Amrhein et al., 2019a, 2019b). Effects and their precision, along with the conclusions based on them, were interpreted continuously and probabilistically, considering data quality, plausibility of effect, and previous literature, all within the context of each outcome (Amrhein et al., 2019a, 2019b; McShane et al., 2019).

3. Results

3.1. MVC and time to momentary failure

Reductions in MVC were not appreciable (i.e., small and with overlapping interval estimates) between the first and second trials, nor between those who completed the trials in a different order (i.e., 30 % vs.

[b] Centre frequencies for the 11 wavelets were respectively 6.90 Hz, 19.29 Hz, 37.71 Hz, 62.09 Hz, 92.36 Hz, 128.48 Hz, 170.39 Hz, 218.08 Hz, 271.50 Hz, 330.63 Hz, and 395.46 Hz as per von Tscharner (2000).

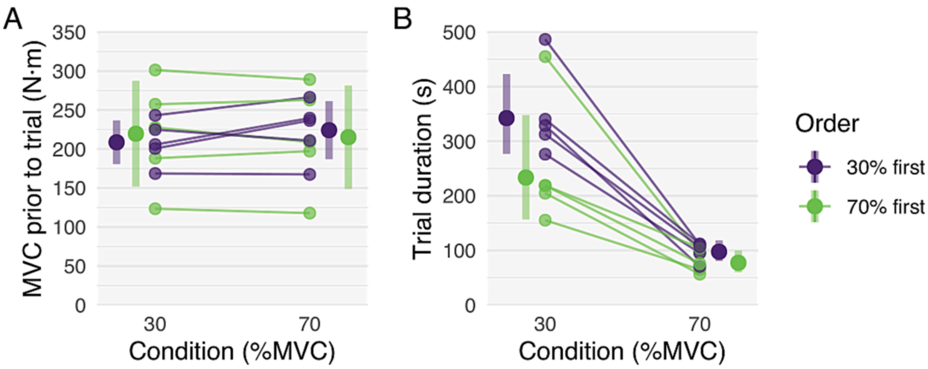

Fig. 1. **(A)** MVC prior to trial and **(B)** trial durations for each participant for the 30 % and 70 % conditions. Thick dots and error bars are mean ± SD in **(A)** and geometric mean ⋇ geometric SD in **(B)** and participants performing the 30 % condition first are shown in purple, and those performing the 70 % condition first are shown in green.

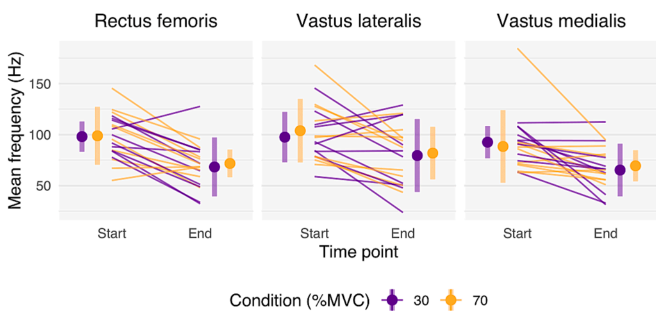

Fig. 2. Start and End mean frequencies for the rectus femoris, vastus lateralis and vastus medialis for each participant Thick dots and error bars are mean ± SD and participants performing the 30 % condition first are shown in purple, while those performing the 70 % condition first are shown in orange.

70 % first) (Fig. 1A). Time-to-momentary failure was, on average, 3.3 ⋇ 1.3 -times longer (geometric mean ⋇ geometric SD) for the low torque trial condition compared with the high torque trial condition. In contrast to the MVCs, there was an order effect for time-to-momentary failure. Specifically, 30 % trial durations were an average of 46 % longer when the 30 % trial preceded the 70 % trial, but the 70 % condition was only 26 % longer when the 70 % trial preceded the 30 % trial (Fig. 1B). Since there was an order effect on trial duration in our sample (not necessarily inferentially), we visually ensured that there was no salient effect of order for other outcomes. These visual checks can be found in our Open Science Framework project (https://osf.io/g2z4w/) in the folder 'supplementary plots'.

3.2. Mean frequency

As calculated from the wavelet transformed signals, there was a decrease in mean frequency from the start to the end of both the low- and high-torque conditions. These frequencies were similar across torque conditions (Fig. 2). This is supported by the mixed-effects models, which showed minimal effects of torque on the mean frequency at momentary failure for the rectus femoris (effect of 70 % relative to 30 % (CI_{95} %)[c] = 3 Hz (−11, 18)), vastus lateralis (2 Hz (−16, 20)), and vastus medialis (4 Hz (−10, 20)).

3.3. sEMG frequency components

At the start of each 30 % condition, the greatest intensities occurred at the lower frequencies, with relatively little signal content at higher frequencies in each muscle (dark blue in Fig. 3). As the trial progresses, intensity increases in the low-to-mid frequency ranges, while greater intensities are also shown to occur in the higher frequency components after approximately 60 % of the trial duration (green-yellow in Fig. 3).

In the 70 % condition, there is initially intensity across all frequencies (note colours extend the whole frequency spectrum in Fig. 3), with the greatest intensities at mid-to-low frequencies. Over the course of the trial, there is an increase in intensity visible in the lower frequencies (note region displaying green-yellow colour in Fig. 3). The higher frequencies' intensity reduction is not as visible in these figures. For example, some loss of intensity can be seen in the highest wavelets at the very end of the trial, particularly in the RF.

3.4. Agreement between signal frequency components

Concordance correlation coefficients increased with respect to the duration of the 30 % trial and either decreased slightly (VM and VL) or remained approximately the same (RF) with respect to the 70 % trial (Table 1, Fig. 4).

3.5. Relative change in signal intensity across frequency domains

In each muscle, the low-torque trials led to an increase in intensity across the whole frequency spectrum studied, but these increases are larger for the lower compared to higher frequencies (Table 2, Fig. 5). In contrast, during the high-torque trials, there was an increase in signal intensity of the lower frequency components, but a decrease in the intensity of the higher frequency components. The transition between increasing and decreasing occurs at different frequencies in the three muscles: ~200 Hz in VM, ~75 Hz in RF, and ~ 150 Hz in VL.

4. Discussion

This appears to be the first study to examine the frequency characteristics of the quadriceps sEMG signal using wavelet-based analysis of sEMG under both high- and low-torque conditions to momentary failure. The mean signal frequency was similar between high- and low-torque conditions at momentary failure. However, an inspection of finer-grained frequency domains (i.e., individual wavelets) reveals that changes differed between frequency components and were a function of the torque condition. These frequency shifts may have several origins and thus require careful interpretation.

The differences in signal intensity changes within the different frequency components—between the high- and low-torque conditions—is

[c] Note, for those not familiar the CIs are reported following the common notation for intervals of numbers between *a* and *b*, including *a* and *b*, and denoted [*a*,*b*] where *a* is the lower CI bound and *b* is the upper CI bound. See, https://en.wikipedia.org/wiki/Interval_(mathematics)#Notations_for_intervals.

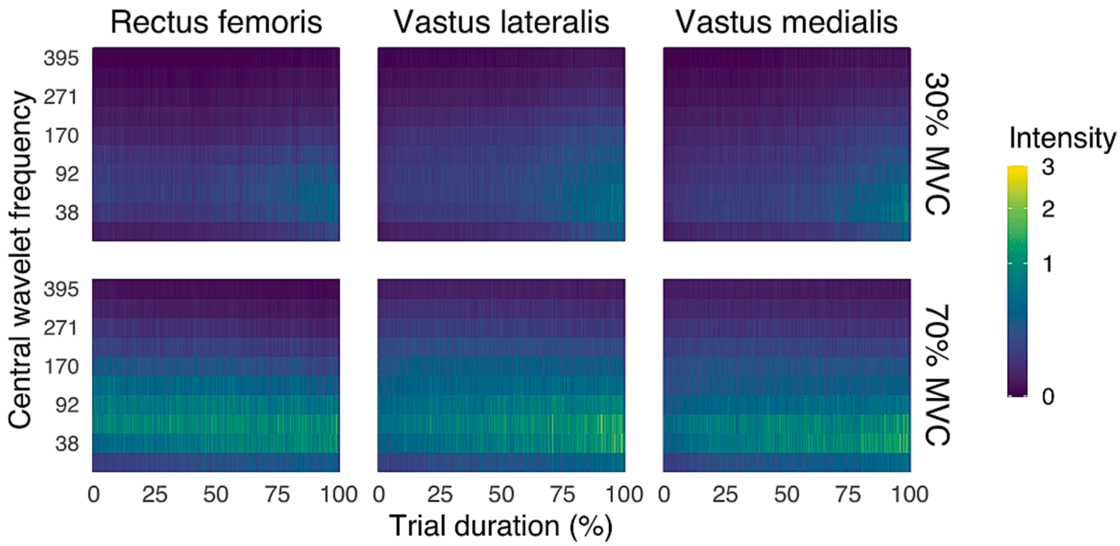

Fig. 3. Spectrograms of wavelet intensities across time. Time is normalised to percentage of trial duration (%) across the *x*-axis; the *y*-axis indicates the wavelet bin number, with higher bin numbers corresponding to higher frequencies. Color indicates intensity of the wavelet bin at a given time point.

Table 1
Relationship between trial durations and the agreement of wavelet intensities.

Muscle	Parameter	Estimate ± SD
Rectus femoris	Intercept	0.09 ± 0.08
	Time of 30 % MVC trial	0.21 ± 0.13
	Time of 70 % MVC trial	0.00 ± 0.13
Vastus lateralis	Intercept	0.11 ± 0.11
	Time of 30 % MVC trial	0.26 ± 0.11
	Time of 70 % MVC trial	−0.08 ± 0.07
Vastus medialis	Intercept	0.09 ± 0.11
	Time of 30 % MVC trial	0.30 ± 0.13
	Time of 70 % MVC trial	−0.07 ± 0.06

Note: Times range from 0 (start of trial) to 1 (end of trial), meaning each intercept is the agreement at $t = 0$ and the slopes represent the average change in the concordance correlation over the duration of the trial (unlike in Fig. 4 where time is normalised from 0 to 100 % of trial duration). SD indicates the standard deviation associated with the random- (or participant level-) effects rather than fixed- (or time level-) effects.

quite striking (Fig. 5). In both cases, there is a relatively greater increase in the low-frequency content compared to high frequencies. This increase could be representative of several physiological factors. However, interpretation specifically regarding MU properties should be made with caution as these changes could equally result from fatigue-related changes in membrane properties that would influence both action potential shape and conduction velocity and, therefore, the signal frequency components (Mortimer et al., 1970; Brody et al., 1991; Dimotrova and Domitrov, 2003; Dideriksen et al., 2011). Given that the increase in lower frequency components is common to both high- and

Table 2
Wavelet intensity intercepts and slopes for each muscle for the 30 % and 70 % conditions.

		Rectus femoris	Vastus lateralis	Vastus medialis
30 % MVC	**Intercept**	1.009 ± 0.003	1.013 ± 0.003	1.020 ± 0.003
	Slope	−0.005 ± 0.001	−0.005 ± 0.001	−0.003 ± 0.001
70 % MVC	**Intercept**	0.993 ± 0.002	0.999 ± 0.002	1.001 ± 0.002
	Slope	−0.009 ± 0.001	−0.007 ± 0.001	−0.005 ± 0.001
Contrast (30–70 %)	**Intercept**	0.016 (0.009, 0.023)	0.014 (0.007, 0.021)	0.019 (0.012, 0.026)
	Slope	0.004 (0.003, 0.005)	0.002 (0.001, 0.003)	0.002 (0.001, 0.003)

Note: Estimates and contrasts are based on estimated marginal means with Satterthwaite degrees-of-freedom approximations. Data are presented as estimate ± SE and estimate ($CI_{95\%}$).

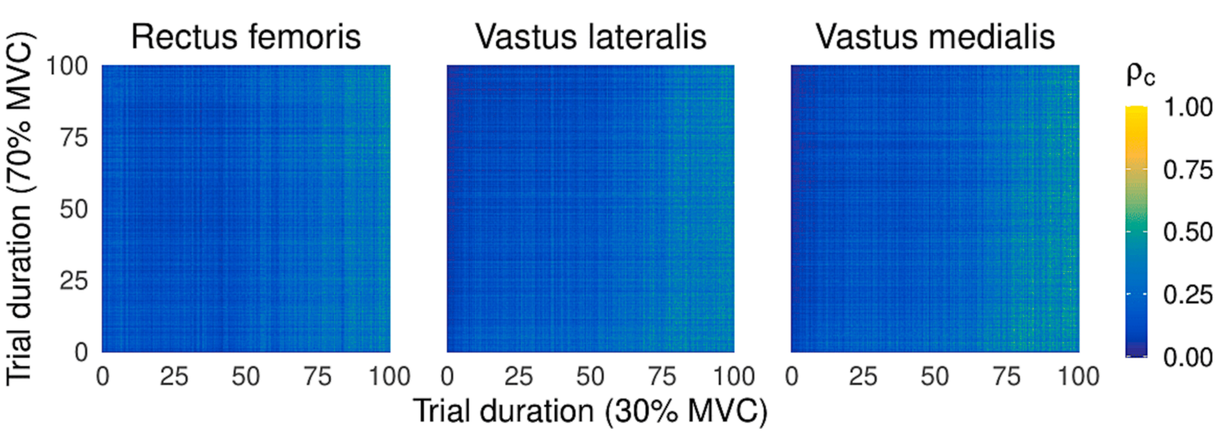

Fig. 4. Average absolute agreement of wavelet intensity vectors across trial durations. Each point represents the average concordance correlation coefficient between the wavelet intensity vector from % of trial duration on the *x* axis for the 30 % trial and % of trial duration on the y axis of the 70 % trial.

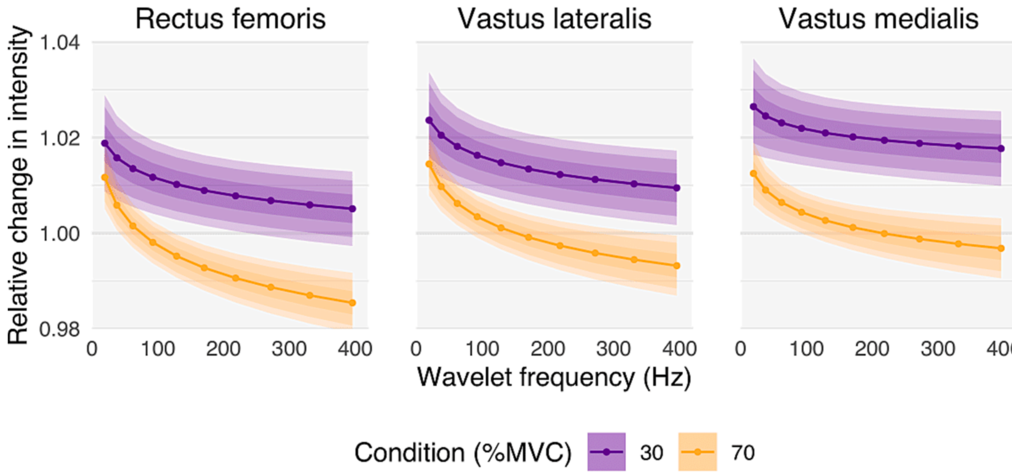

Fig. 5. Relative changes in wavelet intensities across for each muscle for the 30 % and 70 % conditions. Lines and ribbons are from estimated marginal means on the model's fixed effects with Satterthwaite degrees-of-freedom approximation. The ribbons indicate CIs at the 68, 95, and 99 % level, corresponding to approximately 1, 2, and 3 standard errors.

low-torque trials, we can only speculate as to the cause of these changes.

In contrast, relative changes in wavelet intensities differed between conditions. These differences were especially apparent in the higher frequency components in each of the three muscles. Specifically, an increase in relative change across all frequencies was a common feature of each of the three muscles for the low torque trial. In contrast, intensity reductions within the higher frequencies occurred for high torque trials (Fig. 3). The fact that opposite effects were observed between the two conditions indicates that different myoelectric signal properties resulted from the two conditions. Whilst it is tempting to interpret wavelet frequency characteristics as in some way being indicative of MU properties such as recruitment, amplitude cancellation effects occurring primarily at relative torques > 15 % MVC (Dideriksen and Farina, 2019) impact the interpretation of such MU properties (Keenan et al., 2006). Alternatively, this latter effect in the high torque conditions could also be due to changes in action potential shape and conduction velocity from fatigue (Mortimer et al., 1970; Brody et al., 1991) or firing rate adaptations (Potvin & Fuglevand, 2017).[d] Ultimately, due to their nonlinearities and nonstationarities, the exact physiological contributors (e.g., MU recruitment, firing rate, conduction velocity, etc.) to these frequency shifts cannot be ascertained with the methods employed though we hope that our findings prompt such investigations. Future studies should use more sophisticated approaches, such as spike-triggered averaging (Boe et al., 2004) or decomposition using high-density multi-channel electrode arrays (Del Vecchio et al., 2017; Martinez-Valdes et al., 2020), to study the properties of individual motor units.

Our analyses of different frequency components revealed differences between the conditions that could not be identified through amplitude or mean frequency analyses alone. As a point of comparison with our wavelet analyses and with other literature (e.g., Jenkins et al., 2015), we examined the mean frequency across the individual wavelets (Ranniger and Akin, 1997). In the present study, we found that mean frequency decreased similarly across both conditions and muscles. However, our wavelet-based analyses provide further insight into why such mean frequency changes occur which, in this case, were likely a result of the increases in lower frequency components within the signal (Fig. 3). Thus, wavelet-based analysis potentially offers greater insight into how characteristics of the sEMG signal differ between conditions as the trial progresses towards momentary failure. Indeed, upon reaching momentary failure, there was broadly similar frequency content between conditions in our study (Figs. 3 & 4).

Despite our efforts to strictly control our experiment and perform a rigorous analysis, our findings are still prone to natural factors that affect the sEMG signal. Specifically, the signal frequency content of sEMG is affected by many factors (muscle fibre depth and length, pennation angle, cellular environment, temperature, fatigue, motor unit synchronisation). We could control for several of these factors by collecting data on the same day, from the same individuals, with the same electrode placement and joint angle configuration during an isometric effort. Thus, factors relating to muscle anatomy (i.e., muscle fibre depth and length) would have been unlikely to contribute to any differences. However, small changes in pennation angle may have occurred due to tendon creep within trials. Further, although muscle temperature was not measured, participants completed all trials using the same procedures, and due to our randomised, counterbalanced design, this did not likely contribute to differences between conditions.

As mentioned, fatigue can lead to increased low-frequency components in the signal. Yet, our data showed distinct patterns between torque conditions, which were similar across muscles, thus indicating there are different physiological processes underlying the signal characteristics. MU synchronisation, such as when generating forces rapidly, can also lead to alterations in the spectral profile of the myoelectric signals. This phenomenon typically leads to a spike in the 30 Hz region. However, the torque production rate at the trial's beginning did not differ substantially between the two torque conditions, so firing rate could be expected to be similar in each. Further, we used a defined torque threshold to exclude from the analysis the periods of each trial where ramping up/down of torque occurred at the start/end. Additionally, when analyses were re-run with wavelets, but with the 30 Hz data discarded (rather than just the first wavelet), our results were unaffected. As such, it seems the differences in the results do not reflect differences related to firing rate modulations borne out during early ramping, or late ramping down, of torque production during trials.

5. Conclusions

Wavelet-based analysis revealed differences in frequency characteristics of high- and low-torque tasks sEMG signals that more simple analyses have not previously shown. Importantly, the signal characteristics of the low-torque condition became more similar to that of the

[d] Indeed, for comparison we have rerun the model from Potvin and Fuglevand (2017) using the 30% and 70% conditions used in the present study and include these in the supplementary materials. We show the adapted MU strength and firing rates over time for the whole trials and the final 30% of time for the 30% condition trial (supplementary file https://osf.io/9jznr/).

high-torque condition as participants fatigued. This convergence was achieved via divergent frequency changes between conditions. Specifically, patterns of frequency components differed between conditions with high-torque conditions showing high signal intensities across all frequency components initially; most components increased, except high-frequency signal components, which reduced with trial progression. Low-torque conditions demonstrated increases across all frequency components of the signal. However, we caution against specific interpretations from these data regarding MU properties as the signal frequency content of sEMG is potentially affected by many factors (muscle fibre depth and length, pennation angle, cellular environment, temperature, fatigue, motor unit synchronisation). Ultimately, work directly evaluating MU recruitment that accounts for nonstationarities is required to disentangle these complex factors and their influences on frequency characteristics during exercise tasks, and to understand the possible physiological explananda for them.

6. Declarations

Funding: Not applicable.

Availability of data and material: All data and materials are available on the Open Science Framework (https://osf.io/g2z4w/).

Code availability: All code is available on the Open Science Framework (https://osf.io/g2z4w/).

Authors' contributions: JM, JPF, EHT, and JS conceived of the study and design. JM collected all data. ADV performed to statistical analyses. JRP contributed additional materials/modelling. JM and JS prepared the first draft of the manuscript. All authors contributed to interpretation of the results and edited the final manuscript.

Ethics approval: The study was approved by the Centre of Health, Exercise and Sport Science Research Ethics Committee (ID No. 582) meeting the ethical standards of the Helsinki declaration and was conducted within the Sport Science Laboratories at Southampton Solent University.

Consent to participate: All participants provided informed consent to participate.

Declaration of Competing Interest

The authors declare that they have no known competing financial interests or personal relationships that could have appeared to influence the work reported in this paper.

References

Amrhein, V., Greenland, S., McShane, B., 2019a. Scientists rise up against statistical significance. Nature 567 (7748), 305–307. https://doi.org/10.1038/d41586-019-00857-9.

Amrhein, V., Trafimow, D., Greenland, S., 2019b. Inferential statistics as descriptive statistics: there is no replication crisis if we don't expect replication. Am. Stat. 73, 262–270. https://doi.org/10.1080/00031305.2018.1543137.

Boe, S.G., Stashuk, D.W., Doherty, T.J., 2004. Motor unit number estimation by decomposition-enhanced spike-triggered averaging: control data, test-retest reliability, and contractile level effects. Muscle Nerve 29 (5), 693–699.

Brody, L.R., Pollock, M.T., Roy, S.H., De Luca, C.J., Celli, B., 1991. pH-induced effects on median frequency and conduction velocity of the myoelectric signal. J. Appl. Physiol. 71, 1878–1885. https://doi.org/10.1002/mus.20031.

Chapman, M., Larumbe-Zabala, E., Gosss-Sampson, M., Colpus, M., Triplett, N.T., Naclerio, F., 2019. Perceptual, mechanical and electromyographic responses to different relative loads in the parallel squat. J. Strength Cond. Res. 33 (1), 8–16. https://doi.org/10.1519/JSC.0000000000001867.

Del Vecchio, A., Negro, F., Felici, F., Farina, D., 2017. Associations between motor unit action potential parameters and surface EMG features. J. Appl. Physiol. 123 (4), 835–843. https://doi.org/10.1152/japplphysiol.00482.2017.

Dideriksen, J.L., Enoka, R.M., Farina, D., 2011. Neuromuscular adjustments that constrain submaximal EMG amplitude at task failure of sustained isometric contractions. J. Appl. Physiol. 111, 485–494. https://doi.org/10.1152/japplphysiol.00186.2011.

Dideriksen, J.L., Farina, D., 2019 May 3. Amplitude cancellation influences the association between frequency components in the neural drive to muscle and the rectified EMG signal. PLoS Comput. Biol. 15 (5), e1006985.

Dimotrova, N.A., Domitrov, G.V., 2003. Interpretation of EMG changes with fatigue: facts, pitfalls, and fallacies. J. Electromyogr. Kinesiol. 13 (1), 13–36. https://doi.org/10.1016/s1050-6411(02)00083-4.

Duchateau, J., Enoka, R.M., 2011. Human motor unit recordings: Origins and insight into the integrated motor system. Brain Res. 1409, 42–61. https://doi.org/10.1016/j.brainres.2011.06.011.

Farina, D., 2008. Counterpoint: Spectral properties of the surface emg do not provide information about motor unit recruitment strategies and muscle fiber type. J. Appl. Physiol. 105, 1673–1674. https://doi.org/10.1152/japplphysiol.90598.2008a.

Gardner, M.J., Altman, D.G., 1986. Confidence intervals rather than P values: estimation rather than hypothesis testing. Br Med J (Clin Res Ed). 1986.15;292(6522):746-50. doi: 10.1136/bmj.292.6522.746. PMID: 3082422; PMCID: PMC1339793.

Gonzalez, A.M., Ghigiarelli, J.J., Sell, K.M., Shone, E.W., Kelly, C.F., Mangine, G.T., 2017. Muscle activation during resistance exercise at 70% and 90% 1-repetition maximum in resistance trained men. Muscle Nerve 56 (3), 505–509. https://doi.org/10.1002/mus.25509.

Graham, R.B., Wachowiak, M.P., Gurd, B.J., 2015. The assessment of muscular effort, fatigue, and physiological adaptation using EMG and wavelet analysis. PLoS One 10, e0135069.

Hodson-Tole, E.F., Wakeling, J.M., 2007. Variations in motor unit recruitment patterns occur within and between muscles in the running rat (*Rattus norvegicus*). J. Exp. Biol. 210, 2333–2345. https://doi.org/10.1242/jeb.004457.

Hodson-Tole, E.F., Wakeling, J.M., 2009. Motor unit recruitment for dynamic tasks: current understanding and future directions. J. Comp. Physiol. B 179, 57–66. https://doi.org/10.1007/s00360-008-0289-1.

Jenkins, N.D., Housh, T.J., Bergstrom, H.C., Cochrane, K.C., Hill, E.C., Smith, C.M., Johnson, G.O., Schmidt, R.J., Cramer, J.T., 2015. Muscle activation during three sets to failure at 80 vs. 30% 1RM resistance exercise. Eur. J. Appl. Physiol. 115 (11), 2335–2347. https://doi.org/10.1007/s00421-015-3214-9.

Keenan, K.G., Farina, D., Merletti, R., Enoka, R.M., 2006. Amplitude cancellation reduces the size of motor unit potentials averaged from the surface EMG. J Appl Physiol (1985). 2006 Jun;100(6):1928-37. doi: 10.1152/japplphysiol.01282.2005.

Lee, S.S.M., Miara, M.D.B., Arnold, A.S., Biewener, A.A., Wakeling, J.M., 2011. EMG analysis tuned for determining the timing and level of activation in different motor units. J. Electromyogr. Kinesiol. 21 (4), 557–565. https://doi.org/10.1016/j.jelekin.2011.04.003.

Length, L.V., 2020. emmeans: Estimated Marginal Means, aka Least-Squares Means. R package version 1.5.3. 2020. https://CRAN.R-project.org/package=emmeans.

Looney, D.P., Kraemer, W.J., Joseph momentary failure, Comstock, B.A., Denegar, C.R., Flanagan, S.D., Newton, R.U., Szivak, T.K., DuPont, W.H., Hooper, D.R., Häkkinen, K., Maresh, C.M., 2016. Electromyographical and perceptual responses to different resistance intensities in a squat protocol: Does performing sets to failure with light loads produce the same activity? J Strength Cond Res. 30(3):792-799. doi: 10.1519/JSC.0000000000001109.

Lüdecke, D., 2018. ggeffects: Tidy Data Frames of Marginal Effects from Regression Models. J. Open Source Software. 3 (26), 772. https://doi.org/10.21105/joss.00772.

Martinez-Valdes, E., Negro, F., Falla, D., Dideriksen, J.L., Heckman, C.J., Farina, D., 2020 Oct 1. Inability to increase the neural drive to muscle is associated with task failure during submaximal contractions. J. Neurophysiol. 124 (4), 1110–1121. https://doi.org/10.1152/jn.00447.2020.

McShane, B.B., Gal, D., Gelman, A., Robert, C., Tackett, J.L., 2019. Abandon statistical significance. Am. Stat. 73, 235–245. https://doi.org/10.1080/00031305.2018.1527253.

Mortimer, J.T., Magnusson, R., Petersen, I., 1970. Conduction velocity in ischemic muscle: effect on EMG frequency spectrum. Am. J. Phys. Anthropol. 219, 1324–1329. https://doi.org/10.1152/ajplegacy.1970.219.5.1324.

Pinheiro, J.C., Bates, D.M. Linear mixed-effects models: Basic concepts and examples. In. Pinheiro JC, Bates DM. Mixed-Effects Models in S and S-PLUS. Springer, New York. doi: 10.1007/0-387-22747-4_1.

Potvin, J., Fuglevand, A., 2017. A motor-unit based model of muscle fatigue. PLoS Comput. Biol. 13, e1005581.

R Core Team. R: A language and environment for statistical computing. R Foundation for Statistical Computing, Vienna, Austria. URL: https://www.R-project.org/.

Ranniger, C.U., Akin, D.L., 1997. EMG mean power frequency determination using wavelet analysis. Proceedings of the 19th Annual International Conference of the IEEE Engineering in Medicine and Biology Society. 'Magnificent Milestones and Emerging Opportunities in Medical Engineering'. doi: 10.1109/IEMBS.1997.757017.

Schoenfeld, B., Contreras, B., Willardson, J.M., Fontana, F., Tiryaki-Sonmez, G., 2014. Muscle activation during low- versus high-load resistance training in well trained men. Eur. J. Appl. Physiol. 114, 2491–2497. https://doi.org/10.1007/s00421-014-2976-9.

Schoenfeld, B.J., Contreras, B., Vigotsky, A.D., Ogborn, D., Fontana, F., Tiryaki-Sonmez, G., 2016. Upper body muscle activation during low- versus high-load resistance exercise in the bench press. Isokinetics Exerc. Sci. 24 (3), 217–224. https://doi.org/10.3233/IES-160620.

Steele, J., Fisher, J., Giessing, J., Gentil, P., 2017. Clarity in reporting terminology and definitions of set endpoints in resistance training. Muscle Nerve 56 (3), 368–374. https://doi.org/10.1002/mus.25557.

Vigotsky, A.D., 2020. Concordance Correlation and Cross-Correlation Matrices. 2020. *In preparation.*

von Tscharner, V., 2000. Intensity analysis in time-frequency space of surface myoelectric signals by wavelets of specified resolution. J. Electromyogr. Kinesiol. 10 (6), 433–445. https://doi.org/10.1016/s1050-6411(00)00030-4.

von Tscharner, V., 2002. Time-frequency and principal-component methods for the analysis of EMGs recorded during a mildly fatiguing exercise on a cycle ergometer.

J. Electromyogr. Kinesiol. 12 (6), 479–492. https://doi.org/10.1016/s1050-6411(02)00005-6.

von Tscharner, V., Goepfert, B., 2006. Estimation of the interplay between groups of fast and slow muscle fibers of the tibialis anterior and gastrocnemius muscle while running. J. Electromyogr. Kinesiol. 16 (2), 188–197. https://doi.org/10.1016/j.jelekin.2005.07.004.

von Tscharner, V., Nigg, B.M., 2008. Point:Counterpoint: Spectral properties of the surface EMG can characterise/do not provide information about motor unit recruitment strategies and muscle fiber type. J. Appl. Physiol. 105, 1671–1673. https://doi.org/10.1152/japplphysiol.90598.2008.

Wakeling, J.M., 2009a. Patterns of motor unit recruitment can be determined using surface EMG. J. Electromyogr. Kinesiol. 19, 199–207. https://doi.org/10.1016/j.jelekin.2007.09.006.

Wakeling, J.M., 2009b. The recruitment of different compartments within a muscle depends on the mechanics of the movement. Biol. Lett. 5 (1), 30–34. https://doi.org/10.1098/rsbl.2008.0459.

Wakeling, J.M., Pascual, S.A., Nigg, B.M., von Tscharner, V., 2001. Surface EMG shows distinct populations of muscle activity when measured during sustained sub-maximal exercise. Eur. J. Appl. Physiol. 86, 40–47. https://doi.org/10.1007/s004210100508.

Wakeling, J.M., Rozitis, A.J., 2004. Spectral properties of myoelectric signals from different motor units in the leg extensor muscles. J. Exp. Biol. 207, 2519–2528. https://doi.org/10.1242/jeb.01042.

Wilkinson, G.N., Rogers, C.E., 1973. Symbolic description of factorial models for analysis of variance. J. Appl. Stat. 22 (3), 392–399. https://doi.org/10.2307/23467867.